

JGR Biogeosciences

RESEARCH ARTICLE

10.1029/2022JG007161

Key Points:

- We present novel leaf-scale pulse-amplitude modulated (PAM) measurements to study the photosynthetic performance of salt marsh at different inundation levels
- We found the influence of tidal inundation on Spartina alterniflora photosynthetic efficiency varied across the canopy and tide ranges
- We found only 20% of the photosystem II reaction centers in S. alterniflora leaves are open for electron transfer when submerged

Supporting Information:

Supporting Information may be found in the online version of this article.

Correspondence to:

L. Mao, lm53372@uga.edu

Citation:

Mao, L., Mishra, D. R., Hawman, P. A., Narron, C. R., O'Connell, J. L., & Cotten, D. L. (2023). Photosynthetic performance of tidally flooded Spartina alterniflora salt marshes. Journal of Geophysical Research: Biogeosciences, 128, e2022JG007161. https://doi.org/10.1029/2022JG007161

Received 31 AUG 2022 Accepted 22 FEB 2023

Photosynthetic Performance of Tidally Flooded Spartina Alterniflora Salt Marshes

Lishen Mao¹, Deepak R. Mishra¹, Peter A. Hawman¹, Caroline R. Narron¹, Jessica L. O'Connell^{1,2,3}, and David L. Cotten^{1,4}

¹Department of Geography, University of Georgia, Athens, GA, USA, ²Department of Marine Sciences, University of Georgia, Athens, GA, USA, ³Department of Marine Science, Marine Science Institute, University of Texas at Austin, Port Aransas, TX, USA, ⁴Oak Ridge National Laboratory, Oak Ridge, TN, USA

Abstract Spartina alterniflora has a distinct flood-adapted morphology, and its physiological responses are likely to vary with differences in tidal submergence. To understand these responses, we examined the impacts of tidal inundation on the efficiency of Photosystem II (ϕ PSII) photochemistry and leaf-level photosynthesis at different canopy heights through a combination of in situ chlorophyll fluorescence (ChIF), incident photosynthetically active radiation, and tide levels. Our result showed small declines (7%–8.3%) in ϕ PSII for air-exposed leaves when the bottom canopies were tidally submerged. Submerged leaves produced large reductions (30.3%–41%) in ϕ PSII. Our results suggest that when submerged, PSII reaction centers in S. alterniflora leaves are still active and able to transfer electrons, but only at ~20% of the typical daily rate. We attribute this reduction in ϕ PSII to the decrease in the fraction of "open" PSII reaction centers (10% of the total) and the stomatal conductance rate caused by the tidal submergence. To our knowledge, this flooding induced leaf-level reduction of ϕ PSII for S. alterniflora in field settings has not been reported before. Our findings suggest that canopy-level ϕ PSII is dependent on the proportion of submerged versus emerged leaves and highlight the complexities involved in estimating the photosynthetic efficiency of tidal marshes.

Plain Language Summary The photosynthetic performance of coastal marshes, an important blue carbon ecosystem, under tidal flooding has not been extensively studied. Our study aimed to understand and analyze coastal marsh plant photosynthesis under varying tide heights and answer a few fundamental questions related to the differences in the photosynthesis rates between air-exposed and submerged parts of the canopy. Our field observations on the relationship between leaf-level chlorophyll fluorescence of Spartina alterniflora marsh plant and tide levels showed that photochemical efficiency differed markedly based on leaf submergence. Additionally, we observed greatly reduced but active underwater photosynthesis activities in fully submerged leaves, suggesting that S. alterniflora potentially remains a carbon sink during tidal inundation. We conclude that the impact of flooding on leaf-level photosynthesis is driven by their submergence status, and the proportion of emerged and submerged leaves is a significant variable in estimating the photochemical efficiency at the canopy scale. This study can help establish empirical links between canopy chlorophyll fluorescence and carbon fluxes and improve carbon budget estimations at larger scales for these increasingly fragile and important blue carbon ecosystems.

1. Introduction

Tidal marshes are among the most productive ecosystems, and an important carbon (C) sink in the global carbon cycle (Bianchi, 2006). The average C burial rate of coastal salt marshes is as much as 1,713 g C m⁻² yr⁻¹ in sediment, ~35 times higher than in terrestrial forests (McLeod et al., 2011), which provides the key scientific motivation to understand salt marsh productivity across space and time. Salt marshes experience periodic tidal flooding, which affects plant production (Hawman et al., 2021; O'Connell et al., 2021) and photosynthetic rates (Kathilankal et al., 2011). However, only a handful of studies have been conducted to understand photosynthetic behavior under flooded conditions within tidal marshes (Duarte et al., 2005; Kathilankal et al., 2008). Pezeshki et al. (1993) showed that a congener, *Spartina patens*, had a 46% reduction in rates of photosynthesis and 18% reduction in carbon assimilation under hypoxic (flooded) conditions in microcosm experiments. Kathilankal et al. (2008) used field measurements during tidal flooding to demonstrate a 66% reduction in photosynthetic activity of the submerged salt marsh plant, *Spartina alterniflora*, Loisel (*S. alterniflora*) (Kartesz, 2015; USDA & NRCS, 2020) (= *Sporobolus alterniflorus*; Peterson et al., 2014a, 2014b). But this reduced photosynthetic rate

© 2023. American Geophysical Union. All Rights Reserved.

MAO ET AL. 1 of 17

underwater may not translate directly to differences in gas exchanges, as Forbrich and Giblin (2015) found reductions in canopy-level gas exchange from tidal inundation only had a small effect (2%-4%) on seasonal carbon budgets. Because of the variations in results reported by these limited number of studies and their varying scales, more studies are needed to understand salt marsh photosynthetic performance during both high and low tides, i.e., during different levels of plant submergence, to better estimate their primary production budgets. More importantly, studies are needed to answer a few fundamental questions, such as (a) do marsh canopies photosynthesize underwater? (b) if yes, what are their photosynthesis rates? (c) how does the photosynthesis rate vary between air-exposed and submerged parts of the canopy under moderate to high tidal flooding?

This study is aimed at answering the above questions by evaluating the influence of tides on chlorophyll fluorescence (ChIF) and photosynthetic performance in marshes dominated by the salt marsh plant, *S. alterniflora*, a perennial graminoid species tolerant of intermittent tidal flooding and high salinities. *S. alterniflora* is often found in monoculture across broad marsh areas that correspond to its physiological tolerances. We focused on *S. alterniflora* because it is the most common salt marsh plant along the southeastern coast of the United States (Ainouche et al., 2004), and is further found on all three coasts of the conterminous United States and nearly every continent globally as either a native or invasive species. Thus, a better understanding of *S. alterniflora* photosynthesis dynamics is important because of its broad spatial coverage. Further, other common marsh plants also grow in monoculture, such as *S. patens* and *Juncus roemerianus*, two other species that are widespread on the southeastern coast of the United States (Gleason & Zieman, 1981; Smart, 1982), and which respond to similar ecological drivers. Thus, our *S. alterniflora* study is the first step toward understanding more broadly salt marsh photosynthesis dynamics in field settings.

Studies of photosynthesis through leaf-level methods in an intertidal environment are not common (Giurgevich & Dunn, 1979; Kathilankal et al., 2011). Most studies used the CO₂ exchange between salt marshes and the atmosphere measured by eddy covariance systems to passively investigate tidal influences on marsh production at broad scales (Artigas et al., 2015; Bonneville et al., 2008; Forbrich & Giblin, 2015; Kathilankal et al., 2008; Moffett et al., 2010; Morris et al., 2013; Nahrawi et al., 2020; Schäfer et al., 2014). These measurements provide valuable data on canopy-scale dynamics of salt marsh production. However, this essentially solves an inverse problem by measuring CO₂ fluxes to infer photosynthesis under tidal inundation. The reduction in canopy-scale CO₂ exchange is not a direct indicator of the reduction in photosynthesis rates under tidal flooding, instead, it could likely be due to other factors such as laterally exported dissolved CO₂, low diffusion rates of CO₂ between the water column and atmosphere, or reduction in soil respiration by incoming tides (Gålfalk et al., 2013; Kathilankal et al., 2008). Therefore, the eddy covariance tower scale may not be able to accurately reflect leaf-scale dynamics in photosynthesis during tidal inundation.

Recently, satellite-based solar-induced chlorophyll fluorescence (SIF) measurements emerged as a key indicator in studies estimating vegetation photochemical performance and productivity (Frankenberg et al., 2014; Mohammed et al., 2019; Rossini et al., 2010). Studies have found close correlations between satellite SIF, a measurement of passive ChIF during satellite overpass, and gross primary production (GPP) in terrestrial ecosystems, including forests (Yang et al., 2015), croplands (Guanter et al., 2014), and grasslands (Verma et al., 2017) at multiple spatial-temporal scales (Sun et al., 2017; Zhang et al., 2016). These studies provide valuable results on ecosystem-scale vegetation photosynthetic dynamics in response to environmental gradients. However, applying these models to coastal wetlands has so far been limited (Huang et al., 2022) because we lack a comprehensive understanding of leaf-level ChIF-SIF-GPP relationships in ecosystems where tidal flooding or saturated soils introduce uncertainties in the SIF signal, which is a remote sensing measurement similar to spectral reflectance. For example, there are large uncertainties in reflectance measurements caused by canopy submergence during tidal flooding (Ghosh et al., 2016; Kearney et al., 2009; O'Connell et al., 2017), which may decouple reflectance-based models from their ecological underpinnings. In order to have a more reliable and cost-efficient SIF-based GPP estimation for flooded salt marshes at broader scales, there is a critical need to link high-frequency ChlF on leaf level (active) to passive ChlF measurements retrieved from remote sensing platforms (Magney et al., 2017; Meeker et al., 2021). This will allow us to understand the spatiotemporal variability in photosynthetic performance and the associated environmental drivers in salt marshes.

Active measurements of the quantum yield of ChlF with pulse-amplitude modulated (PAM) fluorometry have been used to study the acclimation of the photosynthetic apparatus at the leaf level for several decades (Bilger et al., 1995; Maguire et al., 2020; Porcar-Castell, 2011; Porcar-Castell et al., 2008). ChlF is a key parameter in

MAO ET AL. 2 of 17

studying plant photosynthesis because it carries detailed information about the redox state of photosystem II (PSII) within chloroplasts (Murchie & Lawson, 2013). The underlying mechanism of using ChlF to study the photosynthetic performance is straightforward. Light energy captured by chlorophyll in PSII undergoes three energy dissipation processes, often in combination, such that (a) it can be used to drive photochemistry; (b) it can be lost from PSII as heat, or (c) it can be re-emitted from PSII as ChlF. Because these processes compete for the same light energy and PAM fluorometry is able to instantaneously inhibit the photochemistry of PSII (quenching of the fluorescence signal by plastoquinone reduction) by a high-intensity light pulse, the analysis of the leaf-level ChlF yield measured by PAM fluorometry provides direct, continuous information about changes in photosynthesis resulting from environmental drivers such as tidal flooding.

In this study, we evaluated the applicability of high-frequency leaf-level ChIF measurements from PAM fluorometry to examine the impact of tidal flooding on the photosynthetic processes and dynamics in salt marshes under natural field conditions. Our specific objectives were to (a) evaluate the feasibility of using field-based PAM fluorometry for continuous measurements of ChIF in an intertidal salt marsh; and (b) to study the variations in ChIF parameters and photosynthesis in S. alterniflora marshes under natural solar radiation and variable tidal flooding.

2. Materials and Methods

2.1. Study Site

Our study was conducted on the coast of Georgia on Sapelo Island within the Georgia Coastal Ecosystems Long Term Ecological Research (GCE-LTER) site. Sapelo Island is a state-protected barrier island that contains over 40 ha of salt marsh dominated by a monoculture of *S. alterniflora* (Bortolus et al., 2019). We deployed the PAM fluorometers at the Keenan Field marsh site on the west side of Sapelo Island (Latitude 31.444°, Longitude –81.283°). *S. alterniflora* in this area varies in height along an elevation gradient, with tall-form plants (>100 cm) along the low elevation creekbank, medium (50–100 cm), and short-forms (<50 cm) in intermediate and high marshes, respectively. Medium-form plants are the most typical plants in this area (O'Connell et al., 2019). Our field data were collected from 11 July 2020 to 27 July 2020, in the marsh interior at a tall-form to medium-form ecotone, ~25 m east of the Duplin River, and ~8 m north of the nearest tidal creek. Mean stem heights of our study plants were 110 ± 2.3 cm. The elevation of the study location averaged 72 cm NAVD88 based on centimeter-accurate in situ RTK measurements, which is an intermediate marsh elevation in this area, where elevation ranged from 20 to 110 cm (Alber & O'Connell, 2019). This marsh is flooded twice daily by tides, with typical tidal heights from 0 to 120 cm on the marsh platform (Hawman et al., 2021) and a mean range of 2 m. During the majority of tidal inundation periods, *S. alterniflora* was only partially submerged, and leaves at the top of the canopy were exposed to the atmosphere. During our sampling period, the study site did not experience any disturbance (e.g., hurricane, dieback, wrack deposition).

2.2. Leaf-Scale Chlorophyll Fluorescence Measurements

We used the aquatic version of a monitoring PAM chlorophyll fluorometer to measure leaf-level ChlF (Heinz Walz GmbH, Effeltrich, Germany). The aquatic Monitoring PAM fluorometer consists of one data acquisition logger (MONI-DA/S), one PC interface box (MONI-IB4/USB), and four emitter-detector units (MONI-HEAD/S). They are connected using waterproof data communication cables (RS-485/S). A built-in battery and 500 Megabytes microSD card are sealed within MONI-DA/S, which allows for consistent monitoring of ChlF under frequent flooding conditions (water resistance up to 75 m). MONI-HEAD/S is a compact (~250 g) 3-cm wide by 28-cm long water-tight aluminum cylinder with built-in photosynthetically active radiation (PAR) and temperature sensors. It also has a blue LED light (peak at 455 nm) that is used to deliver measuring light, actinic light, as well as a saturating pulse, which are situated within a sample clip for modulated fluorescence measurements. The leaf clip was mounted at a distance of 2.5 cm and 120° from the lens. We inserted two to three pairs of green and healthy S. alterniflora leaves into each sample clip because a single S. alterniflora leaf, particularly at the top of the canopy, was not wide enough to cover the entire clip. We also placed a black high-density foam behind the sample clip to eliminate background interference. In addition, we added polyurethane (PU) foam at the top and bottom edges of the clip holder to maximumly simulate and promote the seawater flow through the monitored sample leaves and ensure that those leaf samples remained in place for an extended period, in particular during tidal inundation. It also reduced the etiolation symptoms of our monitored leaves as it remained healthy throughout the experiment. The field pictures (Figures S1 and S2 in Supporting Information S1) demonstrate the unchanged conditions of the leaves before and after the deployment. The intensity of measuring light at the sample clip level is adjustable, ranging from 0.1 μmol m⁻² s⁻¹ at low

MAO ET AL. 3 of 17

Figure 1. Field picture of leaf-level ChIF measurement system. (a) A custom-made PVC frame that supports ChIF measurements from Spartina alterniflora at the top and bottom of the plant canopy, and (b) a detailed view of the MONI-HEAD/S installed at 35 cm from the soil surface with a clip to measure S. alterniflora leaves at the bottom of the plant canopy. Note that the S. alterniflora leaves remain healthy in the sample clip.

frequency (5 Hz) to 15 μ mol m⁻² s⁻¹ at high frequency (500 Hz). The same blue LED emits up to 1,500 μ mol m⁻² s⁻¹ actinic light and up to 2 s saturation pulse for maximally 6,000 μ mol m⁻² s⁻¹ at the sample clip level. A filter is used within the lens of MONI-HEAD/S to exclusively isolate the reflected ChIF signal at wavelengths >645 nm.

To ensure robust ChIF measurements during tidal inundation, we built a rectangular PVC frame from 1-inch PVC pipes for MONI-HEAD/S deployment (Figure 1a). Each corner of the rectangular base was secured to the soil by a PVC leg (screwed to the frame and inserted into the soil 60 cm). The two long sides of the base were connected by a PVC pipe (80 cm in length). From the middle of this connector, a central PVC pipe (110 cm in length) rose vertically from the center position of the rectangular base, creating a stable mount for the sensor. We used two MONI-HEAD/S to measure the tidal influences on ChIF of S. alterniflora at two different stem heights: one each at the top of the canopy (TOC) and bottom of the canopy (BOC), ~105 and 35 cm from the soil surface. MONI-HEAD/S were installed on the custom-made PVC frames (Figures 1a and 1b). The position of the top sensor was determined by the marsh plant height (average canopy height was 110 ± 2.3 cm during sampling). The bottom sensor position was determined by the height of the leaves lowest on the plant stem.

ChIF parameters, including maximum ChIF in dark (F_m) and in light (F_m') , minimal ChIF in dark (F_0) , and steady-state fluorescence (F') were measured by each MONI-HEAD/S. The intensity of the measuring light was set as $0.1 \text{ mol m}^{-2} \text{ s}^{-1}$ under "low-frequency" model in light, respectively. The saturation light used maximum photosynthetic photon flux density (PPFD) with 0.8 s integration time. The measuring light switched off after each saturating measurement but automatically switched on before the next saturating pulse. *S. alterniflora* leaves were sampled at 5-min intervals, resulting in 288 data points collected daily, which allowed us to continuously monitor the influence of tides on *S. alterniflora* photosynthetic activities. The final data set included 4,896 observations from each MONI-HEAD/S, with 9,792 observations in total. All measured and derived ChIF parameters are listed in Table 1 and described below.

Fluorescence measurement provides leaf-level information on the acclimation of PSII energy partitioning in a natural environment (Adams & Demmig-Adams, 2004; Baker, 2008; Logan et al., 2007). The F_0 and F_m were measured in the dark-adapted state (i.e., predawn). The maximum quantum yield of PSII was calculated following Maxwell and Johnson (2000) as

$$\frac{F_v}{F_m} = (F_m - F_0)/F_m$$

where F_{ν}/F_{m} indicates the maximal photosynthetic potential of a dark-adapted leaf with no heat dissipation and all reaction centers open.

PSII operating efficiency (φPSII) is the fluorescence parameter that indicates the efficiency at which light is absorbed by PSII. φPSII is used for a light-adapted leaf and estimates photochemistry yield. φPSII was determined following Genty et al. (1989) as:

$$\varphi PSII = (F_v - F')/F'_{to}$$

where $F_{m'}$ is the fluorescence maximum in the light-adapted state, and F' is the fluorescence yield at which the absorbed radiant energy is emitted from the *S. alterniflora* leaf in actinic light conditions. Theoretically, F'

MAO ET AL. 4 of 17

Table 1				
Description of Chlorophyll Fluorescence	Parameters	Used in	This Stud	y

Parameter		Definition	Measurement
	F_0	Minimal fluorescence measured from a leaf in the dark	Measured after dark-adapted leaf exposed to weak measuring light
	F_{m}	Maximum fluorescence measured from a leaf in the dark	Measured after dark-adapted leaf exposed to saturating light pulse
	$F_{\rm v}$	Range in leaf fluorescence during dark conditions	Difference in fluorescence between $F_{\rm m}$ and F_0 : $F_{\rm v} = F_{\rm m} - F_0$
	$F_{\rm v}/F_{\rm m}$	Maximum quantum efficiency of PSII; the range in fluorescence versus maximal fluorescence during dark conditions	Proportion of fluorescence: $F J F_m$
	F	The steady-state level of fluorescence measured from leaf in the ambient actinic light. Sometimes referred to as $F_{\rm t}$ in the literature	Measured under ambient light conditions before any saturating light pulse
	$F_{\rm m}{}'$	Maximum leaf fluorescence measured in the ambient actinic light	Measured under ambient light after the leaf is exposed to saturating light pulse
	$F_{\mathbf{q}}'$	Range in leaf fluorescence from in actinic light	Difference in fluorescence between $F_{m'}$ and $F: F_{q'} = F_{m'} - F'$
	φPSII	PSII operating efficiency: the proportion of light absorbed by PSII that is used for photosynthesis	Proportion of fluorescence between F_q' and F_m' : F_q'/F_m'

Note. The parameter with a prime (') notation represents measurements from the leaf under continuous actinic light that drives photosynthesis. The parameter without a prime represents continuous measurements from the leaf in the dark, where modulated measuring light absorbed by PSII is used completely for photochemistry.

is higher than F_0 as the primary quinone acceptor (Q_A) cannot become maximally oxidized (i.e., PSII reaction centers are not completely open) in light environments (Baker, 2008). In addition, F_m ' should be lower than F_m because of an increase in the efficiency of heat dissipation (i.e., nonphotochemical quenching—NPQ) with increasing light intensity (Murchie & Lawson, 2013).

2.3. Leaf-Scale PPFD Measurements

To carefully examine the impact of tidal inundation on the photosynthetic dynamics of salt marshes, we continuously measured the incident PAR that plants received at different stem heights under natural field conditions. We used LI-192 (LI-COR Biosciences, Lincoln, NE), an underwater quantum sensor that is accurate in air and underwater. To minimize reflectance interference from the instrument frame, upwelling and downwelling quantum sensors were fixed on a black finished metal frame (LI-COR 2009S lowering frame), and then mounted on black painted PVC pipes (1-inch diameter PVC pipes, henceforth expressed as "PAR tree"; Figure 2a). Two PAR trees were deployed to simultaneously measure downwelling PAR at different stem heights of the plant (at 105 and 35 cm from the soil surface, respectively), which corresponds to the heights of the TOC and BOC PAM measurements described previously. The PAR acquisition frequency was programmed to match PAM ChIF data. We then used a waterproof cable (LI-COR 2222UWB) to transmit PAR to a XLite 9210B data logger (Sutron Corporation, Sterling, VA).



Figure 2. Field deployment of quantum and pressure transducer sensors. (a) A set of LI-192 quantum sensors measuring upwelling and downwelling photosynthetically active radiation (PAR) at the top of the marsh with the help of the customized frame. (b) A customized PVC well with fabric cover and infiltration holes which was built to secure Hobo data logger for continuous water height measurements caused by tidal inundation.

MAO ET AL. 5 of 17

We calibrated the PPFD data obtained from underwater quantum sensors (LI-192) for both in-air and underwater conditions. The photon intensity at different plant heights was determined following the factory LI-192 calibration equation: Radiation = Measured Current × Calibration Multiplier. Where the measured current was the output of the sensor in microamps, and the calibration multiplier was a multiplier that distinguishes sensor operating conditions. For example, an underwater multiplier is always greater than an in-air multiplier because of the immersion effect. We applied an immersion coefficient multiplier to the BOC quantum sensor when it was fully submerged. In this context, we postcalibrated 2,186 downwelling measurements from the quantum sensor at BOC with the corresponding tide height and immersion coefficient multiplier. We did not apply underwater multiplier to the TOC measurements because it was never submerged during the sampling.

2.4. Tide Height Measurements and Plant Submergence

We used HOBO U20 Water Level Data Logger (Onset Computer Corporation, Bourne, MA) to record water table heights near the PAM fluorometers. These water table measurements were taken ~4.8 m east of MONI-HEAD/S at an elevation of 0.76 m NAVD88. We placed the sensor in a well (2-inch diameter PVC pipe) that was 120-cm deep under the vegetated marsh soil surface. We drilled infiltration holes every 20 cm on four sides of the PVC well to stimulate groundwater flow. We also used a fabric cloth as a cover to prevent sedimentation (Figure 2b). The HOBO logger was programmed to collect well water level data in 5-min intervals, concurrent with ChIF measurements. We calculated water table height relative to the soil surface for MONI-HEAD/S and "PAR trees" by subtracting the soil surface elevation at the sensor location from the water height. Thus, water table heights below the soil surface are negative.

To determine the influence of tidal inundation on the photosynthetic performance of *S. alterniflora*. We designated three conditions of tidal inundation from the BOC perspective, including fully submerged, partially submerged, and air-exposed. In our study, air-exposed indicates leaves that are exposed to the atmosphere. Fully submerged indicates conditions when the BOC leaves are completely submerged. Partially submerged represents conditions when leaves at the height of BOC sensor are exposed to the atmosphere, but plants below the BOC sensor are fully submerged. This is a transient period for plants between getting submerged in rising tide (tide moves in) and being exposed with the receding tide (tide moves out). TOC leaves were always exposed in the air during our sampling period. We also selected midday flooding that peaked between 10:00 and 16:00 US EST following Kathilankal et al. (2008).

3. Result

3.1. Environmental and Tide Level Data

Daily time courses of tidal inundation over the soil surface are shown in Figure 3a for 11–27 July 2020. A horizontal dashed line indicates tide heights that inundated the BOC MONI-HEAD/S at 35 cm above the soil surface. Two tide peaks were recorded on most days, and tidal flooding rarely exceeded 25 cm above the soil surface during the beginning of sampling (between 11 and 15 July 2020). However, in the latter half of July, the maximum tide height was >45 cm above the soil surface, which covered the base of the stem and submerged the BOC MONI-HEAD/S.

Diurnal dynamics of PAR on TOC and BOC leaves of *S. alterniflora* are shown in Figure 3b for 11-27 July 2020. In general, the diurnal variation in PPFD shows a similar pattern on the TOC and BOC leaves, albeit leaves at BOC receive much fewer photons during midday. For example, during tide inundation on 12 July, air-exposed leaves at TOC received an average $1,449 \pm 52.2$ (mean \pm SD) PPFD compared to 736 ± 35.3 (mean \pm SD) m of photons m⁻² s⁻¹ received by completely submerged leaves at BOC. Results will be presented in the form of mean \pm standard deviation (SD) in the rest of the paper unless otherwise noted.

3.2. Diurnal Leaf-Scale Fluorescence Variations

An example of the continuous TOC and BOC ChIF parameters measured by PAM fluorometers is shown in Figure 4 for 27 July 2020. 27 July was the fourth day in a row when the maximum tide level reached >45 cm over the soil surface. The fluorescence yields observed from leaves in the dark showed differences in the fluorescence yield within the canopy. For example, F_0 measured from the TOC leaves were 2 times greater than BOC leaves

MAO ET AL. 6 of 17

21698961, 2023, 3, Download od from https://agupubs

ibray.wioy.com/doi/10.1029/2022.0007161 by University Of Georgia Libraries, Wiley Online Library on [1000/2023] See the Terms and Conditionary

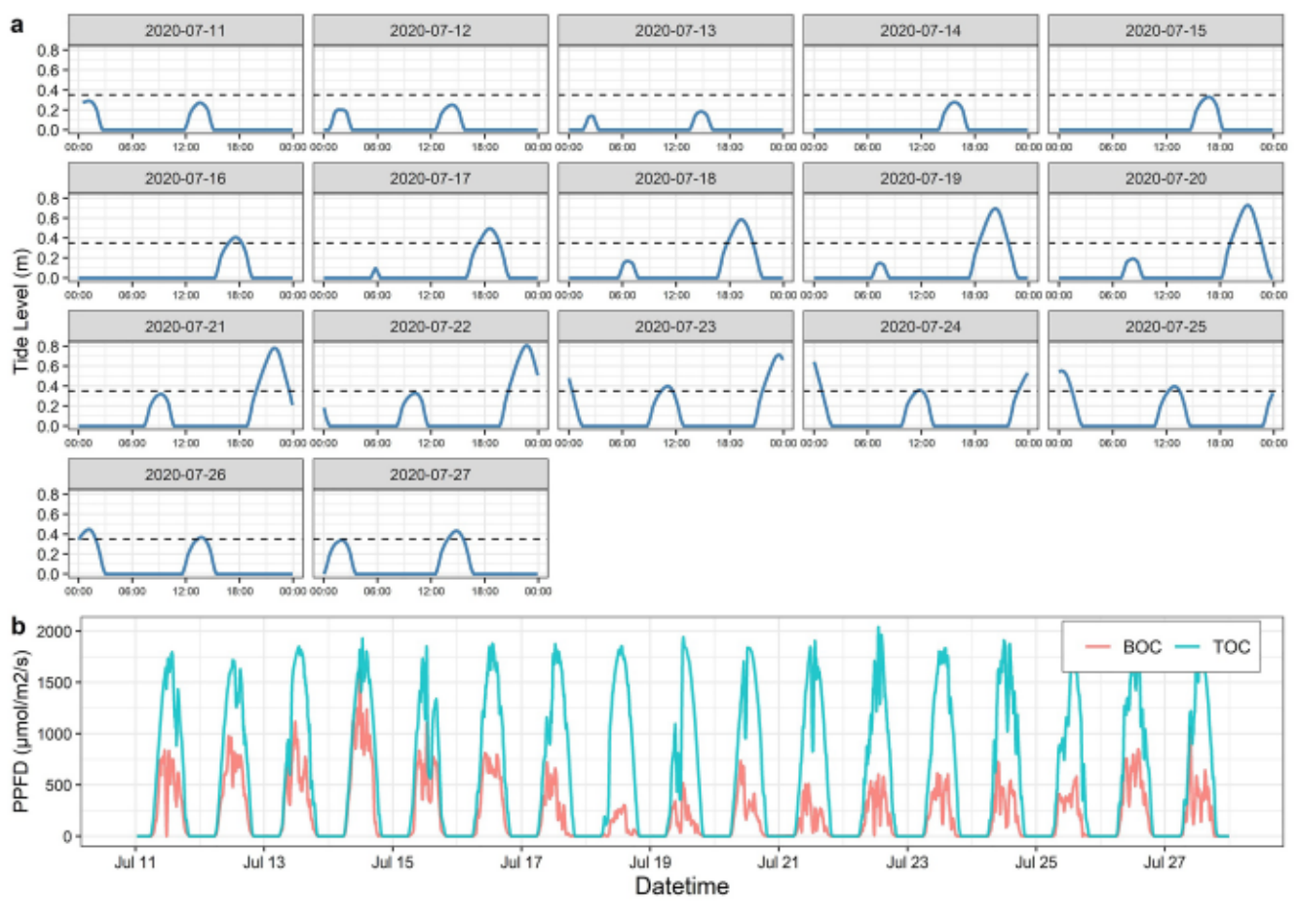


Figure 3. Daily environmental variables collected between 11 and 27 July 2020 from Spartina alterniflora (S. alterniflora) marsh at Sapelo Island, GA: (a) The blue line represents the daily tide cycle and highlights the tide level of each peak tide over the soil surface (= 0 cm). The dashed horizontal line indicates the deployment position of emitter-detector sensor (MONI-HEAD/S) at the bottom of the canopy (BOC), which becomes completely submerged when tide height is >35 cm from the soil surface. Note that the top of canopy MONI-HEAD/S at 105 cm, were never submerged during the study. (b) The green and red lines illustrate the diurnal change pattern and peak of photosynthetic photon flux density (PPFD) incident on TOC and BOC leaves of S. alterniflora, respectively. BOC Leaves received diminished PPFD compared to leaves at TOC. The low PPFD for the BOC sensor on 18 July is most likely due to increased light attenuation from higher turbidity observed at the nearest NOAA National Estuarine Research Reserve System (NERRS) water quality monitoring station data (not shown).

(TOC F_0 range: 200.25 \pm 4.14; BOC F_0 range: 102.47 \pm 3.75). F_m measurements followed a similar ratio, with higher TOC F_m and lower BOC F_m (TOC $F_m = 906 \pm 2.74$; BOC $F_m = 469 \pm 2.83$). However, we found similar F_m (mean = 0.78) on both TOC and BOC leaves (Figure 4a).

Diurnal variations of F' and $F_{\rm m'}$ illustrate responses of PSII to within canopy differences in the natural environment (i.e., natural light and heat stress) (Table 2). The TOC F' and $F_{\rm m'}$ variations can be grouped into three general stages (Figure 4b). First, after sunrise (TOC PAR > 0), $F_{\rm m'}$ started decreasing immediately, and F' rose sharply with a corresponding reduction in $F_{\rm m'}$. These phenomena denote that the TOC leaves are highly sensitive to PPFD and heat increases after sunrise, indicated by a decrease in $F_{\rm m'}$. However, a decrease in the ability to oxidize $Q_{\rm A}$, indicated by a larger increase in F' (Table 2), is the main factor that determines the change of φ PSII after sunrise (Baker, 2008; Maguire et al., 2020). Second, both $F_{\rm m'}$ and F' changed in a similar fashion during the day despite tidal inundation at the BOC. For example, F' and $F_{\rm m'}$ stayed relatively constant with an average midday range of 459 ± 11 and 614 ± 17 , respectively. The lowest $F_{\rm m'}$ occurred in the early afternoon ($F_{\rm m'} = 571$ at 13:05), when the ambient air temperature was 31.59°C, and light radiation was intense at 1,953 μ mol m⁻² s⁻¹. This daytime change pattern of fluorescence yields in S. alterniflora during flooding is similar to those that were reported in *Pinus sylvestris*, *Fagus sylvatica*, and *Cucurbita pepo* (Bilger et al., 1995; Porcar-Castell, 2011; Porcar-Castell et al., 2008). Therefore, all of these observations illustrate that fluorescence yields at the top of the marsh canopy are only slightly affected by tidal flooding as long as the top of the canopy is air-exposed, even

MAO ET AL. 7 of 17

oambloi/10.1029/2022/2007/161 by University Of Georgia Librarias, Wiley Online Library on [10/03/2023] See the Term

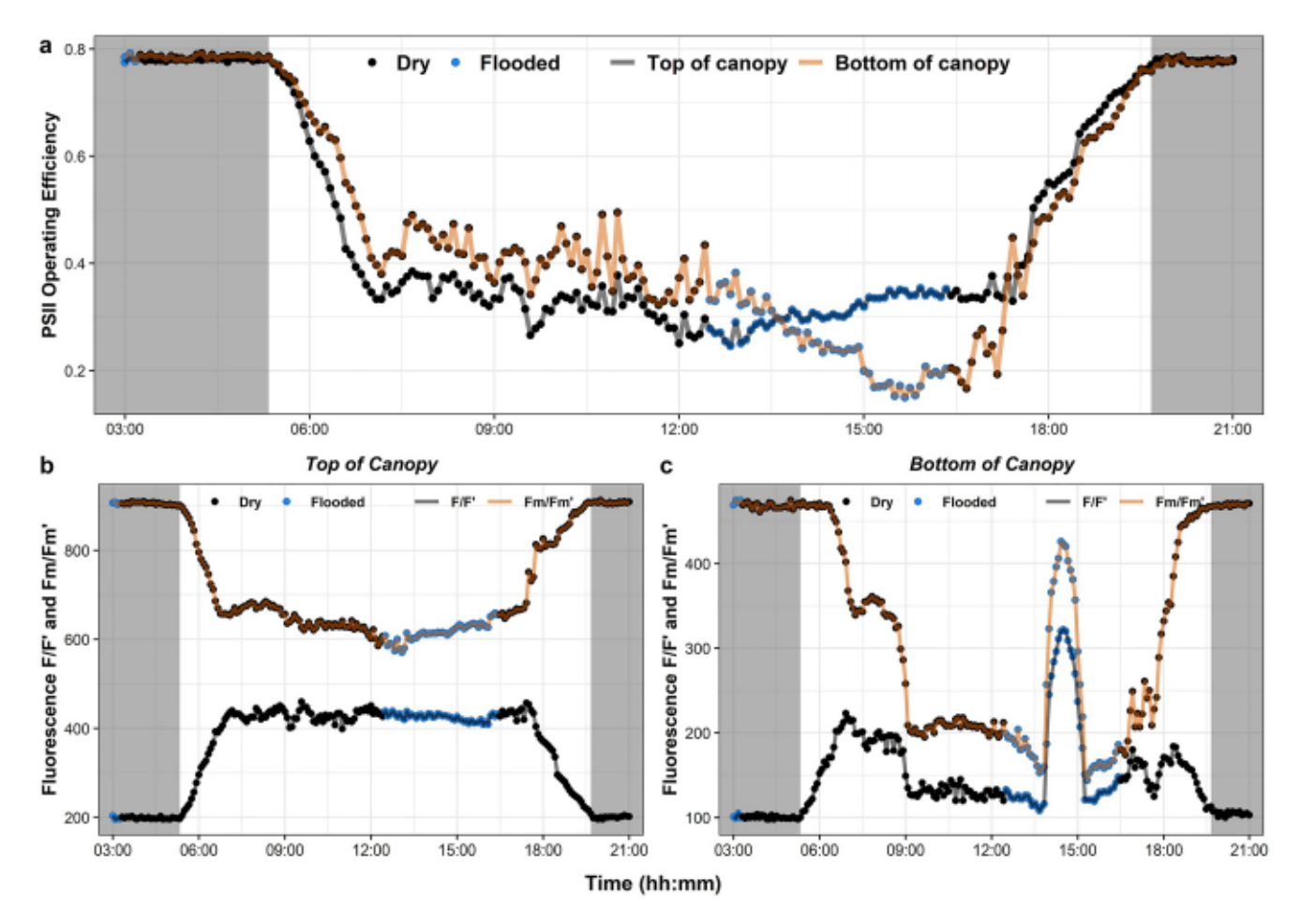


Figure 4. Diurnal dynamics of chlorophyll fluorescence (ChlF) parameters observed at 5-min intervals during a high tide period that occurred in the middle of the day on 27 July 2020: (a) PSII operating efficiency (ϕ PSII) at the top of the canopy (TOC) (105 cm, solid line) and bottom of the canopy (BOC) (35 cm, dotted line); (b and c) maximum ChlF (dotted line) and current ChlF emissions (become F_0 at night) (solid line) observed from the TOC and BOC, respectively. Blue points indicate the variation in ChlF parameters during tidal flooding when the maximum tide height was 45 cm above the soil surface, which should significantly submerge the BOC sensor head. The shaded area indicates nighttime observations when photosynthetic photon flux density (PPFD) = 0, a prime (') notation used after Chl parameters that represent daytime measurements when photosynthesis is occurring.

at times when the BOC is submerged. Third, in the early evening, both F' and $F_{\mathfrak{m}'}$ experienced recovery with a steady decline of F' and a constant rise in $F_{\mathfrak{m}'}$. This recovery was almost completed before darkness when the measurements of F' and $F_{\mathfrak{m}'}$ reached close to F_0 and $F_{\mathfrak{m}}$, respectively. No obvious fluctuations in fluorescence yields were observed at night.

Table 2
Summary of Variation of Averaged Chlorophyll Fluorescence (ChlF) Measurements After Dawn ($0 < PAR < 266 \ \mu mol \ m^{-2} \ s^{-1}$)
During the Entire Sampling Period

	Parameters	Dawn (0 < PPFD < 10)	Early morning (10 < PPFD < 266)	% Change of ChlF after dawn
Top of the canopy (TOC)	F'	207 ± 31	442 ± 68	+113%
	$F_{\mathrm{m}}{}'$	877 ± 54	678 ± 98	-22%
Bottom of the canopy (BOC)	F'	109 ± 32	182 ± 56	+67%
	$F_{\mathrm{m}}{}'$	458 ± 22	334 ± 87	-27%

Note. F' measured at the top of S. alterniflora canopy increased by 113% on average after sunrise, while simultaneously, $F_{m'}$ decreased on average by 22%. Overall, F' and $F_{m'}$ measurements from the BOC present similar patterns of variation with the TOC observations after dawn but with differences in the magnitude of fluctuation. The unit of PAR is μ mol m⁻² s⁻¹.

MAO ET AL. 8 of 17

com/doi/10.1029/2022/20007161 by University Of Georgia Libraries, Wiley Online Library

Table 3

Variation of PSII Operating Efficiency (φPSII) at the Top (TOC) and Bottom (BOC) of the Spartina Alterniflora (S. Alterniflora) Canopy During (a) High Tide and (b) Low Tide Flooding

		High tide flooding					
a	TOC				BOC		
Tide height	0-35 cm	≥35 cm	Dry*	0-35 cm	≥35m	Dry*	
Submergence	Air-exposed	Air-exposed	Air-exposed	Partially submerged	Fully submerg	ged Air-exposed	
φPSII (mean ± SD)	0.28 ± 0.03	0.28 ± 0.03	0.30 ± 0.03	0.33 ± 0.06	0.23 ± 0.05	0.39 ± 0.05	
% Changes	-7.0%*	-7.0%*		-15.4%*	-30.3% -	-41%*	
		Low tide flooding					
b		TOC		BOC			
Tide height		0-25 cm	Dr	y*	0-25 cm	Dry*	
Submergence		Air-exposed	Air-ex	posed	Partially submerged	Air-exposed	
φ PSII (mean \pm SD)		0.33 ± 0.03	0.36	±0.04	0.34 ± 0.04	0.40 ± 0.05	
% Changes		-8.3%*			-15.0%*		

Note. Changes (%) in φPSII for S. alterniflora leaves between air-exposed, partially submerged, and fully dry (nonflooded) conditions during high tide when the maximum tide height fully submerged BOC MONI-HEAD/S and during low tide when both TOC and BOC MONI-HEAD/S were air-exposed during the maximum tide. Asterisks (*) denote percent change from nonflooded conditions in φPSII at different tide heights. There were pronounced reductions in φPSII in partially or fully submerged S. alterniflora leaves compared to nonflooded conditions. We observed <10% changes in φPSII in air-exposed TOC during both tidal events.

Diurnal variation of fluorescence yields at the BOC also had three general stages, but it was more complex and variable due to the influence of tidal inundation, which sometimes submerged the BOC leaves (Figure 4c). First, after sunrise, F' increased immediately, but $F_{m'}$ stayed constant and started decreasing about 1 hr later. Second, fluorescence yields at the BOC present similar patterns of variation with the daytime TOC observations but with differences in the magnitude of fluctuation. For example, F' and $F_{m'}$ stayed steady within the range of 127 \pm 4.5 and 207 ± 10, respectively, before tidal flooding (Figure 4c). However, tidal inundation led to large fluctuations in fluorescence yields in the BOC leaves. For example, on 27 July 2020, the tide started rising at 12:35, peaked at 14:35, at a height that submerged the BOC leaves, and then gradually decreased until it completely subsided at about 16:25. When tides were highest, a maximal F_m of 426, which is close to F_m , was observed. F' also rose sharply to a maximum that was above even the highest F' from the morning observation period. Water from tidal flooding is a good absorber of both light and heat energy. Thus, the cool, low light environment provided during BOC flooding likely corresponds to minimal levels of NPQ, with the concomitant closure of the majority of PSII reaction centers that would likewise prohibit photochemistry. Thus, most of the light energy absorbed by PSII was lost as ChlF during this time. Third, in the early evening, F' and $F_{m'}$ started returning to levels close to those before sunrise. Although in situ ChlF measurements have been reported for salt marshes (Kathilankal et al., 2008), our time series of daily ChlF dynamics, for the first time, provides continuous leaf-level information on the acclimation of PSII to realistic field tide inundation in S. alterniflora at different canopy heights.

Figure 4a depicts the variation of F_v/F_m and ϕ PSII calculated from the TOC and BOC ChIF. In general, during the high tide day, BOC ϕ PSII was higher than TOC ϕ PSII. For example, the mean BOC ϕ PSII, excluding midday tidal inundation, was 0.39 ± 0.05 compared to the TOC ϕ PSII of 0.3 ± 0.03 (Table 3). During tidal inundation, there were no detectable changes in TOC ϕ PSII, but the BOC leaves showed considerable reductions in ϕ PSII, as it gradually decreases with the increased height of tidal flooding with minimal values below 0.2 during the complete submergence. This is a new finding, and to our knowledge, these differences in leaf-level reductions in ϕ PSII across different S. alterniflora stem heights at different stage of tidal inundation field conditions have not been reported before in the literature.

Photochemical efficiency was influenced by tidal inundation and submergence, as shown by plots of the relative changes in fluorescence yields against NPQ (Figure 5a) and percentage of open PSII reaction center (qL) against φPSII from bottom of S. alterniflora leaves (Figure 5b). We observed low NPQ and high fluorescence yields, particularly when tides >35 cm fully submerged the leaf surface. φPSII and qL were positively related as the tide level increased which eventually led to rapid declines in φPSII and qL. We also observed that underwater

MAO ET AL. 9 of 17

oznáda/10.1029/2022/0007161 by University Of Georgia Librarias, Wiley Online Library on [10/03/2023] See the Term

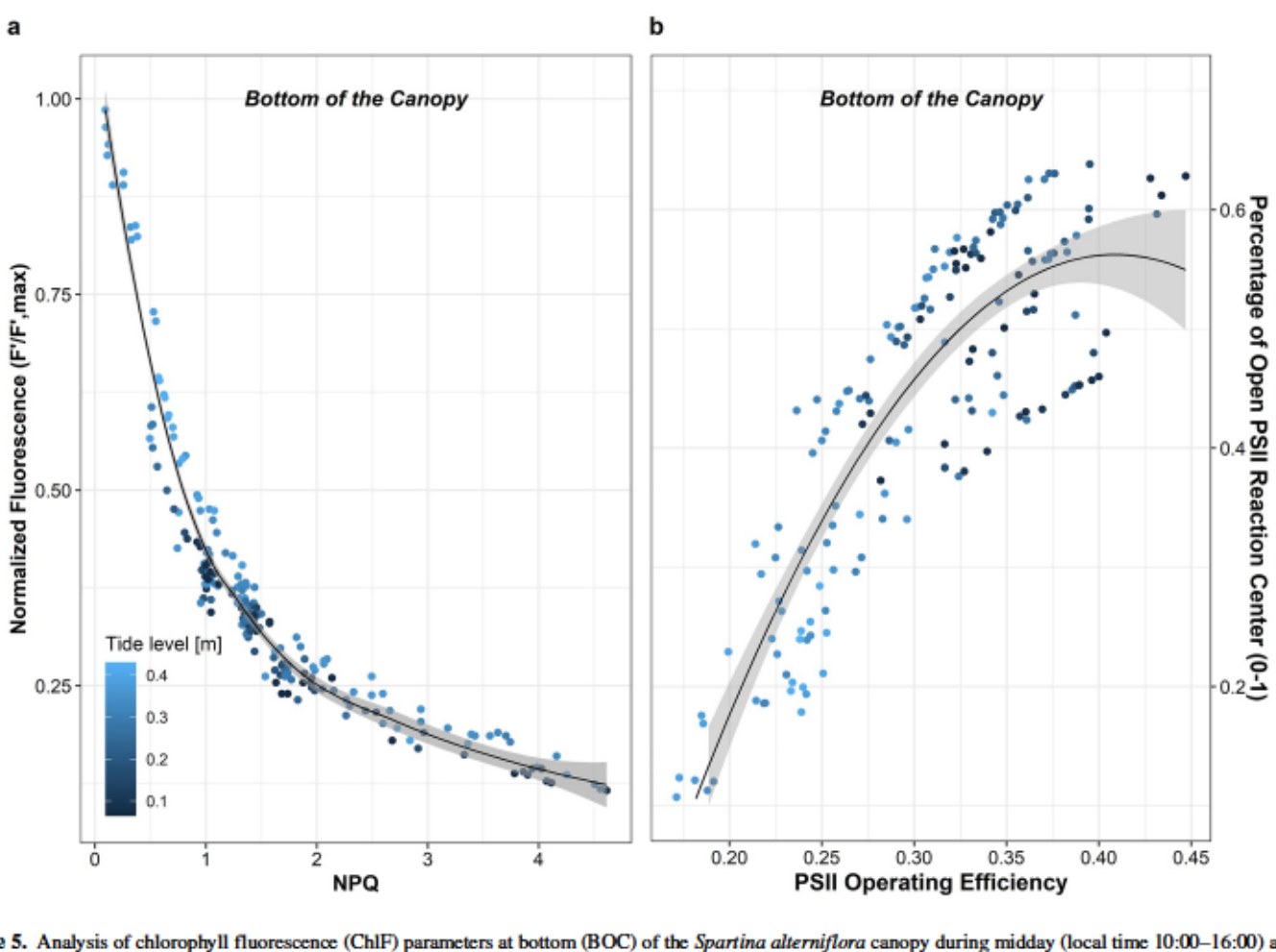


Figure 5. Analysis of chlorophyll fluorescence (ChIF) parameters at bottom (BOC) of the Spartina alterniflora canopy during midday (local time 10:00-16:00) and high tidal flooding. (a) Relationship between steady-state fluorescence yield (F') and nonphotochemical quenching (NPQ), (b) relationship between the fraction of "open" PSII reaction centers (qL) and quantum efficiency of PSII (φ PSII) for BOC S. alterniflora leaves. Lighter blue points indicate a higher tide level above the soil surface. In (a), a low NPQ and high fluorescence yield is observed during high tide level. In (b) underwater photochemistry was observed at a greatly reduced rate accompanied by partially opened PSII reaction centers during high tidal flooding. The φ PSII and qL are also positively associated. Polynomial smoothing lines with 95% confidence intervals (gray areas) were fitted for trend visualization purposes. Observations of F' were normalized to the maximum in the light (F', max) following Magney et al. (2017).

photochemistry rates were greatly reduced and accompanied by partially opened PSII reaction centers. This suggests that PSII reaction centers in fully submerged S. alterniflora leaves were still active and transferring electrons, but only at $\sim 20\%$ of the typical daily rate.

Averaged F_V/F_m for the *S. alterniflora* leaves from TOC and BOC showed a similar value of F_V/F_m at 0.78 (TOC: 0.78 \pm 0.002; BOC: 0.78 \pm 0.004), which is slightly lower than the optimal value reported for many plant species (Bilger et al., 1995; Björkman & Demmig, 1987; Murchie & Lawson, 2013; Yang et al., 2017). To our knowledge, this F_V/F_m has not been reported before for *S. alterniflora* in real-field conditions either. F_V/F_m is thought to reflect the maximum quantum efficiency because leaf-level fluorescence parameters were continuously measured through the night when Q_A was supposed to be maximally oxidized, and the level of heat loss from PSII (NPQ) should have disappeared completely (Maxwell & Johnson, 2000). However, we found that NPQ stayed more or less active at night during our sampling period (averaged night-time NPQ = 0.086 \pm 0.013), which lowered F_m and resulted in a smaller F_V/F_m . This phenomenon has been reported before and described as a common occurrence during summer months with higher night temperatures (Porcar-Castell et al., 2008; Yang et al., 2017). Those conditions represent our site well, where summer nights in coastal Georgia, USA are typically warm and humid. In addition, photoinhibition caused by frequent saturating pulses from PAM fluorometer may have led to a decrease in F_m , resulting in a smaller F_V/F_m at night (Porcar-Castell et al., 2008).

MAO ET AL. 10 of 17

dai/10.1029/2022/2007 161 by University Of Georgia Librarias, Wiley Online Library on [10/03/2023] See the

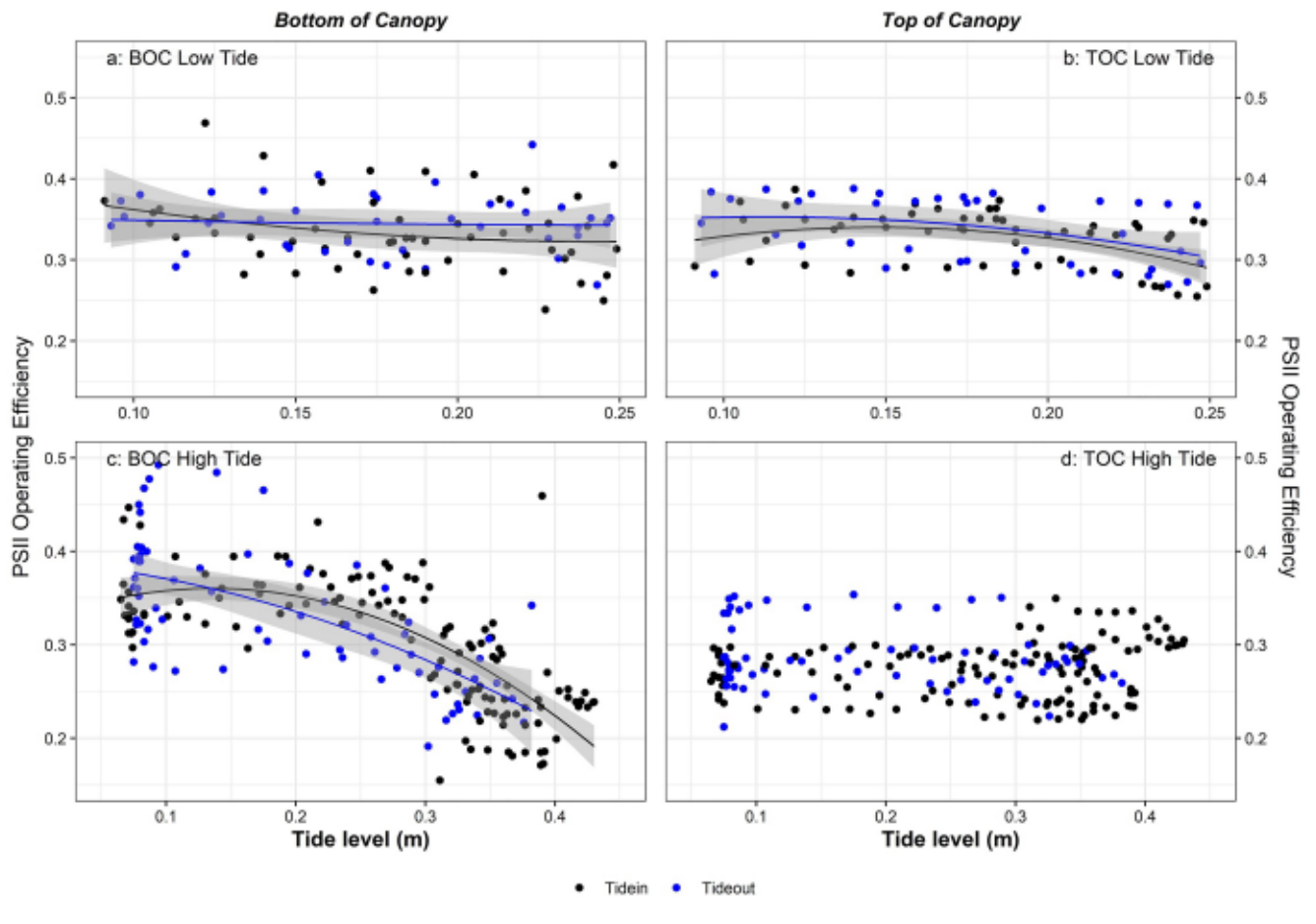


Figure 6. The responses of photosystem II operating efficiency (φPSII) at the (a), (c) bottom (BOC, 35 cm) and (b), (d) top (TOC, 105 cm) of the Spartina alterniflora canopy to increasing water table height during (a), (b) low tide days with 25-cm peak tide level and high tide days with >45-cm peak tide level above the soil surface. Black solid points are φPSII observed during rising tide (tide in), and blue solid points are φPSII measured during receding tide (tide out). Second-degree polynomial smoothing lines with 95% confidence intervals (gray areas) were fitted for trend visualization purposes. There were no sizable changes in φPSII at the top of the S. alterniflora canopy during both tidal events. Substantial changes in φPSII at both canopy heights were also not detected during low tide flooding. However, the BOC φPSII was significantly reduced when BOC leaves were completely submerged by the tide.

3.3. Response of PSII Working Efficiency(\(\phi\)PSII) to Tide Heights

The effect of tidal flooding on ϕ PSII was observed during the daytime. The measured ϕ PSII was plotted against tide height when flooding occurred between 10:00 a.m. and 16:00 p.m. and tide heights did not reach the BOC sensor (Figures 6a and 6b), and when the BOC sensor was completely submerged during flooding (Figures 6c and 6d). On low tide days (peak tide height at ~25 cm), our data did not show substantial fluctuations of TOC and BOC ϕ PSII.

On higher tide days, the BOC ϕ PSII showed sizable reductions as they were negatively associated with tide height (Figure 6c). For example, BOC leaves ϕ PSII dropped from an average of 0.39 ± 0.05 in air-exposed conditions from the start of the tide (nonflooded) to 0.33 ± 0.06 , in partially submerged conditions as the tide level gradually rose (tide height <0.35 cm). The relationship became more pronounced when the tide height > 35 cm completely covered BOC *S. alterniflora* leaves. This resulted in a greatly reduced ϕ PSII rate in fully submerged leaves. For example, the rate of BOC ϕ PSII for fully submerged leaves declined on average by 41% compared to air-exposed leaves in nonflooded conditions (Table 3). In contrast, the impact of high flooding on ϕ PSII in air-exposed TOC leaves was low, with <10% decline on average, at times when the BOC leaves were completely submerged.

In summary, the results demonstrate the applicability of PAM fluorometry to continuously track photochemical and nonphotochemical PSII quantum yields in salt marshes in the field under a range of tidal and light conditions. Our field observations on the relationship between leaf-level S. alterniflora ChIF and tide levels showed that

MAO ET AL. 11 of 17

Journal of Geophysical Research: Biogeosciences

photochemical efficiency differed markedly based on leaf submergence. The rate of φ PSII in fully submerged BOC leaves decreased significantly compared to air-exposed leaves due to the physiological stresses induced by tidal inundation. For example, the lower diffusion rate of gases and increased rate of stomatal closure act as major restrictions for fully submerged leaves (Heinsch et al., 2004; Knox et al., 2018), suggesting that underwater φ PSII is PQ instead of NPQ-limited. Additionally, we observed greatly reduced underwater photosynthesis activities in fully submerged leaves, suggesting that *S. alterniflora* could potentially remain a CO₂ sink during tidal inundation.

4. Discussion

4.1. Spartina Alterniflora Continued to Photosynthesis When Submerged During Tidal Inundation

Our observational study of natural field conditions demonstrated that *S. alterniflora* continued photosynthesis during tidal inundation. Our findings are supported by rigorous PAM ChlF measurements on *S. alterniflora* BOC and TOC leaves and quantitatively relate photosynthetic activities of submerged leaves to the physiological characteristics of *Spartina* plants (Figure 5). For example, when leaves were fully submerged by tides > 35 cm (e.g., the BOC sensor height), we showed that NPQ dropped rapidly to near 0 accompanied by a simultaneous increase in fluorescence yields (Figure 5a). Thus, NPQ was not a determining factor in underwater photosynthesis. Further, light levels were also sufficient for submerged leaves as fluorescence emitted significantly during tidal flooding, suggesting that APAR was more than sufficient to drive photosynthesis. In this context, the observed photosynthetic activity of submerged BOC *S. alterniflora* depends on the fraction of "open" PSII reaction centers. This was supported by Figure 5b, which shows that φPSII and qL are positively related. Figure 5b also suggests that a small portion of PSII reaction centers (~10%) still remained open and carried out photochemistry under complete submergence. These field observations are similar to *S. alterniflora* laboratory experiments conducted by Pezeshki et al. (1993).

During tidal submergence, our results suggest an up to 41% reduction in BOC φPSII when compared to nonflooded conditions (Table 3). However, TOC air-exposed leaves had small reductions in φPSII (7%-8.3%) during tidal inundation of the lower canopy, which was consistent as tides rose, though tides never submerged the upper leaves (Table 3). Additionally, our results suggest that φPSII for fully submerged BOC leaves is 18% lower than the air-exposed TOC leaves during a flooding event. These results highlight the different influences of tidal inundation on photosynthetic processes at the bottom and top of the canopy. To our knowledge, we are the first to report this for intertidal salt marshes. The different influence of tides on φPSII reduction indicates that photosynthesis in TOC and BOC leaves is independent of each other. Further, tidal flooding only causes significant reductions when leaves are actively submerged. Considering the φPSII of the entire canopy as a whole, a 25-cm tide height lead to a 23.3% decrease in φPSII. A 45-cm tide height doubles the φPSII reduction (48%). These estimates are derived from plant-level \(\phi PSII \) decreases observed by combined TOC and BOC sensors during flooded versus nonflooded conditions (Tables 3a and 3b). Previous studies by Kathilankal et al. (2008) reported a much higher 66% reduction in photosynthetic ability for submerged S. alterniflora in Virginia tidal marshes. Their study may have overestimated the impact of tidal inundation because air-exposed and partially submerged plants should experience less reductions in \(\phi PSII. \) Further, tides which completely submerge marsh plants are less common than partially flooded conditions (Hawman et al., 2021; Narron et al., 2022; O'Connell et al., 2017, 2019). Our ChIF measurements similarly suggested that TOC and BOC have independent and different responses of leaf photosynthesis during inundation, and is linked to tidal stage and amplitudes. This also provides new insights into estimating the efficiency of energy partitioning of S. alterniflora PSII throughout the canopy because the submerged/emerged leaf proportion also changes during tidal inundation.

4.3. Impacts of φPSII Variations During Tidal Flooding on Canopy-Scale Studies

The impact of flooding on leaf-level photosynthesis is driven by submergence status, as discussed in Section 4.1. Therefore, the proportion of tide:plant height is a significant variable in estimating photochemical efficiency at the canopy scale (e.g., see Section 4.2). Although not the same type of measurements, our findings are aligned with data presented by many previous studies on the influence of tidal flooding on CO₂ fluxes or net ecosystem

MAO ET AL. 12 of 17

exchange (NEE) or GPP, which have shown decreases in marsh carbon exchange under tidal inundation at ecosystem-scale. For example, Moffett et al. (2010) found a substantial decrease in CO₂ fluxes for S. alterniflora in a California marsh when the tide depth exceeded 17 cm above the ground. Forbrich and Giblin (2015) showed a tide depth above 5 cm could lead to a reduction in marsh productivity. We could not find any study linking in situ ChlF to CO₂ fluxes or Eddy tower scale NEE or GPP for wetlands. It may likely be due to various challenges involved in continuously capturing leaf-level φPSII variations at different plant heights under realistic field tidal inundation. But, we can assume that the variability in in situ ChlF due to tidal inundation would have an impact on CO₂ fluxes or GPP because many prior studies have shown ChlF as a strong indicator of seasonal variability and phenology of GPP in other terrestrial vegetative ecosystems (Flexas et al., 2002; Joiner et al., 2013).

However, our findings bring new complexities to studies involving passive measurements of photosynthesis proxies (e.g., SIF) or carbon assimilation rates (e.g., NEE and GPP via Eddy flux tower) because photosynthesis in fully submerged *S. alterniflora* leaves continuing at reduced rates does not directly link to active gas exchange underwater. This link is needed because we do not know whether marsh species such as *S. alterniflora* internally recycle CO₂ and O₂ (Gleason & Dunn, 1982) produced through photosynthesis, photorespiration, and respiration; or whether they significantly exchange gases with the water column while submerged (Silva et al., 2005; Winkel et al., 2011); or a combination of the two. Once these uncertainties are better understood, we expect methodological revisions will be necessary for canopy-scale NEE calculations and partitioning models (i.e., submerged versus emerged canopies) to estimate GPP and ecosystem respiration for tidal wetlands. These new methods would need to quantify canopy submergence and link it with augmented rates of photosynthesis and gas exchange during tidal flooding.

4.4. Limitations

Our observations of the tidal flooding impact on opPSII for S. alterniflora, whether during low tide or high tide, is limited by sensor reliability, sensor deployment height, the maximum tide height, and inundation duration time. For example, midday high tides with heights that exceeded the BOC sensor (~35 cm) were observed on only 5 days (23-27 July). In addition, the maximum tide height was ~45 cm above the soil surface, which prevented us from studying fully submerged TOC φPSII responses, as these never occurred. In this context, our BOC leaves also were not inundated for extended periods, as tide depth fluctuated within the 4-4.5 hr flooding window. Therefore, this study could not measure the response to continuous and sustained inundation for PSII reaction centers, though we expect that the rate of closure increases with inundation status as light and CO2 become scarce. Morris et al. (2013) reported a greater photosynthetic rate from air-exposed TOC S. alterniflora during a high midday tide of long duration. However, our results show that reductions in \(\phi SII \) began when tide height approached 30 cm, 5 cm below the BOC sensor (Figure 6c). We anticipate that the whole plant φPSII reduction will increase once a threshold flooding level is exceeded. This is because TOC oPSII will likely have a greater reduction when the plant becomes partially or fully submerged. We need more ChIF measurements that demonstrate the vertical distribution of photosynthetic efficiency. Such data would further help to estimate canopy-scale marsh photosynthesis with differing tidal amplitudes, ranges, depths, and durations. However, the conditions during the sampling were representative of the most typical flood patterns at our site. Our observations suggest the photosynthetic efficiency does not change significantly as long as the majority of the canopy is air-exposed during low-level tidal flooding.

4.5. Future Applications

To better understand the photoche mistry and carbon assimilation rates (e.g., GPP) of salt marshes that are frequently inundated, it is essential to understand how changes in in situ photochemical activities are affected by tide-induced submergence of leaf area. If empirical relationships between canopy-scale ChlF parameters representing photochemistry and GPP can be established in future studies, our method can be coupled with gas exchange measurements from Eddy covariance flux towers or radiant retrieval of ChlF from passive sensors (e.g., SIF). That would allow for further assessment of the influence of tidal inundation on marsh photosynthesis and how it affects carbon flux budgets at larger scales. There are several advantages associated with PAM fluorometry-based ChlF data to further understand the dynamics and drivers of underwater canopy photosynthesis. First, automated PAM fluorometry is suitable for field deployment. The instrument also provides continuous and high temporal resolution maximal and minimal fluorescence measurements ($F_{\rm m}$ and $F_{\rm 0}$) when the photosynthetic apparatus is fully relaxed at night. Accurate field-based determination of $F_{\rm m}$ and $F_{\rm 0}$ allows for the quantification of NPQ, $F_{\rm v}/F_{\rm m}$, and photochemical quenching (PQ), which are normally difficult to acquire. Second, automated PAM fluorometry provides reliable measurements under complicated field conditions, such as in tidal wetlands with soft ground and saturated

MAO ET AL. 13 of 17

soils. Third, PAM MONI-HEAD/S observe the same set of leaves and move together with them, which maximally reduces the effects of sample clip and allows for consistent measurements and interpretations for an extended period. Fourth, automated PAM fluorometry can support up to 7 MONI-HEAD/S, which can collect simultaneous ChIF measurements of seven independent leave samples over a 400 m² spatial scale. The footprint of our ChIF monitoring system is limited by cable length, but it is comparable to a flux tower footprint or MODIS 500-m pixel to develop empirical relationships. This feature will be particularly useful in scaling up leaf-level photosynthesis variations within flux tower footprints and connecting to satellite measurements at larger spatial scales.

These results can further our understanding of fluctuations of photosynthesis, SIF spectral shapes, and GPP in salt marshes observed during tidal flooding at multiple scales. Our controlled in situ measurements of leaf-scale ChIF provide fundamental information that can explain vertical differences in the PSII working mechanism and how they may drive ChIF-SIF-GPP relationship observed at longer temporal scales. Our results, which showed a greatly reduced oPSII with the closure of PSII reaction centers and stomata during tidal flooding, offer further explanation for the results observed by Nahrawi et al. (2020) and Hawman et al. (2021). Their studies showed a significant decline in CO, assimilation rates and light use efficiency (LUE) in S. alterniflora during tidal flooding from a flux tower scale. Although, we do not have direct evidence of the occurrence of gas exchange in the submerged canopy of the marsh plant, we can assume overall canopy-level C assimilation is reduced during tidal flooding due to the reduction in PSII levels. Therefore, the satellite data and/or models derived NEE and GPP estimates from salt marshes should be adjusted to include the daily temporary fluctuations in gas exchange during tidal flooding along with other components such as hydrologic exports (Bogard et al., 2020). Hawman et al. (2021) further showed environmental factors, including air temperature, vapor pressure deficits, solar radiation, and tides affect LUE and GPP of S. alterniflora. All of those environmental variables could also be used in future studies to model and predict φPSII for marsh canopies so that φPSII predictions can be scaled to sites where in situ ChIF measurements are unavailable. Future studies should also examine these phenomena in marshes dominated by other common species, such as J. roemerianus and S. patens, which respond to similar environmental gradients.

5. Conclusions

This study presented high temporal resolution field measurements of leaf-scale chlorophyll fluorescence, PSII operating efficiency, and PAR using preprogrammed PAM chlorophyll fluorometer and underwater quantum sensors, to better understand the photosynthetic response of the dominant salt marsh plant, S. alterniflora to tidal inundation. We collected the measurements using a novel system design that was deployed at the top (~105 cm) and bottom (~35 cm) of the S. alterniflora and under a range of tidal amplitudes. Our leaf-level ChIF measurements demonstrated the variation of leaf ChIF and photosynthetic activities in air-exposed, partially submerged, and fully submerged Spartina plants across a range of tidal cycles and differing tidal amplitudes. We found the influence of tidal inundation on S. alterniflora photosynthesis was independent and different in the leaves across the canopy. The observed differences could be explained by differences in meteorological and physiological stresses between the two sampling locations induced by changes in leaf submergence conditions. On days with high tidal flooding, the φ PSII of BOC leaves decreased with increasing tide height. This reduction became more pronounced (up to 41%) when the tide height exceeded 35 cm, completely submerging BOC leaves compared to nonflooded conditions. However, <10% reductions were observed in φPSII of air-exposed leaves at times when the BOC leaves were completely submerged. Additionally, we observed underwater photosynthesis at a greatly reduced rate, accompanied by partially opened PSII reaction centers and low NPQ in fully submerged S. alterniflora leaves during tidal flooding. We quantified that φPSII of fully submerged S. alterniflora leaves was still at 20% capacity compared to air-exposed conditions because at least 10% of PSII reaction centers remained open and carried out photochemistry under complete submergence. These findings suggest that S. alterniflora could potentially remain a CO2 sink during tidal inundation but at greatly reduced rates. We concluded that the plant submergence status should be considered a significant factor in estimating salt marsh photosynthesis. Thus, to create high quality carbon assimilation models for intertidal salt marshes, researchers need to determine the proportion of plant submergence and corresponding PSII operating efficiency of salt marshes before scaling to larger regional studies.

Data Availability Statement

Data that support the findings of this study are available on the GCE-LTER Data Catalog: Sapelo Island leaf-level chlorophyll fluorescence data and other environmental variables (Mao, 2023). Data set summary is also available at https://gce-lter.marsci.uga.edu/public/app/dataset_details.asp?accession=MSH-GCET-2302.

MAO ET AL. 14 of 17

Acknowledgments

This project was supported by NASA Carbon Cycle Science Grant (#NNX17AI76G) and the Georgia Coastal Ecosystems LTER's National Science Foundation funding (OCE-1237140 and OCE-1832178). This is contribution 1111 of the University of Georgia Marine Institute. The authors would like to thank Dontrece Smith, Jacob Shalack, Alvssa Peterson, John Williams, and Elise Diehl for their assistance in field transportation, field data collection, and sensor maintenance at the GCE-LTER site. The authors would like to thank Wade Sheldon, and Adam Sapp for data management at the GCE-LTER site. The authors also thank Dr. Hailong Huang for his help in the first deployment and testing of the PAM fluorometry.

References

- Adams, W. W., & Demmig-Adams, B. (2004). Chlorophyll fluorescence as a tool to monitor plant response to the environment. In G. C. Papageorgiou, & Govindjee (Eds.), Chlorophyll a fluorescence: A signature of photosynthesis (pp. 583-604). Springer.
- Ainouche, M. L., Baumel, A., Salmon, A., & Yannic, G. (2004). Hybridization, polyploidy and speciation in Spartina (Poaceae). New Phytologist, 161(1), 165–172. https://doi.org/10.1046/j.1469-8137.2003.00926.x
- Alber, M., & O'Connell, J. L. (2019). Elevation drives gradients in surface soil temperature within salt marshes. Geophysical Research Letters, 46, 5313–5322. https://doi.org/10.1029/2019GL082374
- Artigas, F., Shin, J. Y., Hobble, C., Marti-Donati, A., Schäfer, K. V. R., & Pechmann, I. (2015). Long term carbon storage potential and CO₂ sink strength of a restored salt marsh in New Jersey. Agricultural and Forest Meteorology, 200, 313–321. https://doi.org/10.1016/j.agrformet.2014.09.012
- Baker, N. R. (2008). Chlorophyll fluorescence: A probe of photosynthesis in vivo. Annual Review of Plant Biology, 59(1), 89–113. https://doi.org/10.1146/annurev.arplant.59.032607.092759
- Bianchi, T. S. (2006). Biogeochemistry of estuaries. Oxford University Press.
- Bilger, W., Schreiber, U., & Bock, M. (1995). Determination of the quantum efficiency of photosystem II and of non-photochemical quenching of chlorophyll fluorescence in the field. Oecologia, 102(4), 425–432. https://doi.org/10.1007/BF00341354
- Björkman, O., & Demmig, B. (1987). Photon yield of O₂ evolution and chlorophyll fluorescence characteristics at 77 K among vascular plants of diverse origins. Planta, 170(4), 489–504. https://doi.org/10.1007/BF00402983
- Bogard, M. J., Bergamaschi, B. A., Butman, D. E., Anderson, F., Knox, S. H., & WindhamMyers, L. (2020). Hydrologic export is a major component of coastal wetland carbon budgets. Global Biogeochemical Cycles, 34, e2019GB006430. https://doi.org/10.1029/2019GB006430
- Bonneville, M.-C., Strachan, I. B., Humphreys, E. R., & Roulet, N. T. (2008). Net ecosystem CO₂ exchange in a temperate cattail marsh in relation to biophysical properties. Agricultural and Forest Meteorology, 148(1), 69–81. https://doi.org/10.1016/j.agrformet.2007.09.004
- Bortolus, A., Adam, P., Adams, J. B., Ainouche, M. L., Ayres, D., Bertness, M. D., et al. (2019). Supporting Spartina: Interdisciplinary perspective shows Spartina as a distinct solid genus. Ecology, 100(11), e02863. https://doi.org/10.1002/ecy.2863
- Duarte, C. M., Middelburg, J. J., & Caraco, N. (2005). Major role of marine vegetation on the oceanic carbon cycle. Biogeosciences, 2(1), 1–8. https://doi.org/10.5194/bg-2-1-2005
- Flexas, J., Bota, J., Escalona, J., Sampol, B., & Medrano, H. (2002). Effects of drought on photosynthesis in grapevines under field conditions: An evaluation of stomatal and mesophyll limitations. Functional Plant Biology, 29(4), 461. https://doi.org/10.1071/PP01119
- Forbrich, I., & Giblin, A. E. (2015). Marsh-atmosphere CO₂ exchange in a New England salt marsh. Journal of Geophysical Research: Biogeosciences, 120, 1825–1838. https://doi.org/10.1002/2015JG003044
- Frankenberg, C., O'Dell, C., Berry, J., Guanter, L., Joiner, J., Köhler, P., et al. (2014). Prospects for chlorophyll fluorescence remote sensing from the Orbiting Carbon Observatory-2. Remote Sensing of Environment, 147, 1–12. https://doi.org/10.1016/j.rse.2014.02.007
- Gålfalk, M., Bastviken, D., Fredriksson, S., & Arneborg, L. (2013). Determination of the piston velocity for water-air interfaces using flux chambers, acoustic Doppler velocimetry, and IR imaging of the water surface. *Journal of Geophysical Research: Biogeosciences*, 118, 770–782. https://doi.org/10.1002/jgrg.20064
- Genty, B., Briantais, J.-M., & Baker, N. R. (1989). The relationship between the quantum yield of photosynthetic electron transport and quenching of chlorophyll fluorescence. Biochimica et Biophysica Acta, 990(1), 87–92. https://doi.org/10.1016/S0304-4165(89)80016-9
- Ghosh, S., Mishra, D. R., & Gitelson, A. A. (2016). Long-term monitoring of biophysical characteristics of tidal wetlands in the northern Gulf of Mexico—A methodological approach using MODIS. Remote Sensing of Environment, 173, 39–58. https://doi.org/10.1016/j.rse.2015.11.015
- Giurgevich, J. R., & Dunn, E. L. (1979). Seasonal patterns of CO₂ and water vapor exchange of the tall and short height forms of Spartina alterniflora Loisel in a Georgia salt marsh. Oecologia, 43(2), 139–156. https://doi.org/10.1007/BF00344767
- Gleason, M. L., & Dunn, E. L. (1982). Effects of hypoxia on root and shoot respiration of Spartina alterniflora. In V. S. Kennedy (Ed.), Estuarine comparisons (pp. 243–253). Academic Press.
- Gleason, M. L., & Zieman, J. C. (1981). Influence of tidal inundation on internal oxygen supply of Spartina alterniflora and Spartina patens. Estuarine, Coastal and Shelf Science, 13(1), 47-57. https://doi.org/10.1016/S0302-3524(81)80104-1
- Guanter, L., Zhang, Y., Jung, M., Joiner, J., Voigt, M., Berry Joseph, A., et al. (2014). Global and time-resolved monitoring of crop photosynthesis with chlorophyll fluorescence. Proceedings of the National Academy of Sciences of the United States of America, 111(14), E1327–E1333. https://doi.org/10.1073/pnas.1320008111
- Hawman, P. A., Mishra, D. R., O'Connell, J. L., Cotten, D. L., Narron, C. R., & Mao, L. (2021). Salt marsh light use efficiency is driven by environmental gradients and species-specific physiology and morphology. *Journal of Geophysical Research: Biogeosciences*, 126, e2020JG006213. https://doi.org/10.1029/2020JG006213
- Heinsch, F. A., Heilman, J. L., McInnes, K. J., Cobos, D. R., Zuberer, D. A., & Roelke, D. L. (2004). Carbon dioxide exchange in a high marsh on the Texas Gulf Coast: Effects of freshwater availability. Agricultural and Forest Meteorology, 125(1), 159–172. https://doi.org/10.1016/j. aerformet.2004.02.007
- Huang, Y., Zhou, C., Du, M., Wu, P., Yuan, L., & Tang, J. (2022). Tidal influence on the relationship between solar-induced chlorophyll fluorescence and canopy photosynthesis in a coastal salt marsh. Remote Sensing of Environment, 270, 112865. https://doi.org/10.1016/j. res. 2021.112865.
- Joiner, J., Guanter, L., Lindstrot, R., Voigt, M., Vasilkov, A. P., Middleton, E. M., et al. (2013). Global monitoring of terrestrial chlorophyll fluorescence from moderate-spectral-resolution near-infrared satellite measurements: Methodology, simulations, and application to GOME-2. Atmospheric Measurement Techniques, 6(10), 2803–2823. https://doi.org/10.5194/amt-6-2803-2013
- Kartesz, J. T. (2015). The biota of North America program (BONAP). North American Plant Atlas, 412, 413.
- Kathilankal, J. C., Mozdzer, T. J., Fuentes, J. D., D'Odorico, P., McGlathery, K. J., & Zieman, J. C. (2008). Tidal influences on carbon assimilation by a salt marsh. Environmental Research Letters, 3(4), 044010. https://doi.org/10.1088/1748-9326/3/4/044010
- Kathilankal, J. C., Mozdzer, T. J., Fuentes, J. D., McGlathery, K. J., D'Odorico, P., & Zieman, J. C. (2011). Physiological responses of Spartina alterniflora to varying environmental conditions in Virginia marshes. Hydrobiologia, 669(1), 167–181. https://doi.org/10.1007/s10750-011-0681-9
- Kearney, M., Stutzer, D., Turpie, K., & Stevenson, J. (2009). The effects of tidal inundation on the reflectance characteristics of coastal marsh vegetation. *Journal of Coastal Research*, 25, 1177–1186. https://doi.org/10.2112/08-1080.1
- Knox, S. H., Windham-Myers, L., Anderson, F., Sturtevant, C., & Bergamaschi, B. (2018). Direct and indirect effects of tides on ecosystem-scale CO₂ exchange in a brackish tidal marsh in Northern California. *Journal of Geophysical Research: Biogeosciences*, 123, 787–806. https://doi. org/10.1002/2017JG004048

MAO ET AL. 15 of 17

Logan, B., Adams, W., & Demmig-Adams, B. (2007). Viewpoint: Avoiding common pitfalls of chlorophyll fluorescence analysis under field conditions. Functional Plant Biology, 34(9), 853. https://doi.org/10.1071/FP07113

Journal of Geophysical Research: Biogeosciences

- Magney, T. S., Frankenberg, C., Fisher, J. B., Sun, Y., North, G. B., Davis, T. S., et al. (2017). Connecting active to passive fluorescence with photosynthesis: A method for evaluating remote sensing measurements of Chl fluorescence. New Phytologist, 215(4), 1594–1608. https://doi. org/10.1111/nph.14662
- Maguire, A. J., Eitel, J. U. H., Griffin, K. L., Magney, T. S., Long, R. A., Vierling, L. A., et al. (2020). On the functional relationship between fluorescence and photochemical yields in complex evergreen needleleaf canopies. Geophysical Research Letters, 47, e2020GL087858. https:// doi.org/10.1029/2020GL087858
- Mao, L. (2023). Pulse amplitude modulated (PAM) 5-minute chlorophyll fluorescence (ChlF) with accompanying environmental variables from the GCE-LTER Keenan field site on Sapelo Island, GA in July 2020. Georgia coastal ecosystems LTER project. University of Georgia, Long Term Ecological Research Network. https://doi.org/10.6073/pasta/93dad8f2c88a1f6b40cef5ed45724acf
- Maxwell, K., & Johnson, G. N. (2000). Chlorophyll fluorescence—A practical guide. Journal of Experimental Botany, 51(345), 659–668. https://doi.org/10.1093/jexbot/51.345.659
- McLeod, E., Chmura, G. L., Bouillon, S., Salm, R., Björk, M., Duarte, C. M., et al. (2011). A blueprint for blue carbon: Toward an improved understanding of the role of vegetated coastal habitats in sequestering CO₂. Frontiers in Ecology and the Environment, 9(10), 552–560. https://doi.org/10.1890/110004
- Meeker, E. W., Magney, T. S., Bambach, N., Momayyezi, M., & McElrone, A. J. (2021). Modification of a gas exchange system to measure active and passive chlorophyll fluorescence simultaneously under field conditions. AoB Plants, 13(1), plas066. https://doi.org/10.1093/aobpla/ plas066
- Moffett, K. B., Wolf, A., Berry, J. A., & Gorelick, S. M. (2010). Salt marsh-atmosphere exchange of energy, water vapor, and carbon dioxide: Effects of tidal flooding and biophysical controls. Water Resources Research, 46, W10525. https://doi.org/10.1029/2009WR009041
- Mohammed, G. H., Colombo, R., Middleton, E. M., Rascher, U., van der Tol, C., Nedbal, L., et al. (2019). Remote sensing of solar-induced chlorophyll fluorescence (SIF) in vegetation: 50 years of progress. Remote Sensing of Environment, 231, 111171. https://doi.org/10.1016/j. rse.2019.04.030
- Morris, J., Sundberg, K., & Hopkinson, C. (2013). Salt marsh primary production and its responses to relative sea level and nutrients in estuaries at Plum Island, Massachusetts, and North Inlet, South Carolina, USA. Oceanography, 26(3), 78–84. https://doi.org/10.5670/oceanog.2013.48
- Murchie, E. H., & Lawson, T. (2013). Chlorophyll fluorescence analysis: A guide to good practice and understanding some new applications. Journal of Experimental Botany, 64(13), 3983–3998. https://doi.org/10.1093/jxb/ert208
- Nahrawi, H., Leclerc, M. Y., Pennings, S., Zhang, G., Singh, N., & Pahari, R. (2020). Impact of tidal inundation on the net ecosystem exchange in daytime conditions in a salt marsh. Agricultural and Forest Meteorology, 294, 108133. https://doi.org/10.1016/j.agrformet.2020.108133
- Narron, C. R., O'Connell, J. L., Mishra, D. R., Cotten, D. L., Hawman, P. A., & Mao, L. (2022). Flooding in Landsat across Tidal Systems (FLATS): An index for intermittent tidal filtering and frequency detection in salt marsh environments. *Ecological Indicators*, 141, 109045. https://doi.org/10.1016/j.ecolind.2022.109045
- O'Connell, J. L., Alber, M., & Pennings, S. C. (2019). Microspatial differences in soil temperature cause phenology change on par with long-term climate warming in salt marshes. *Ecosystems*, 23(3), 498–510. https://doi.org/10.1007/s10021-019-00418-1
- O'Connell, J. L., Mishra, D. R., Alber, M., & Byrd, K. B. (2021). Berm: A belowground ecosystem resiliency model for estimating Spartina alterniflora belowground biomass. New Phytologist, 232(1), 425–439. https://doi.org/10.1111/nph.17607
- O'Connell, J. L., Mishra, D. R., Cotten, D. L., Wang, L., & Alber, M. (2017). The Tidal Marsh Inundation Index (TMII): An inundation filter to flag flooded pixels and improve MODIS tidal marsh vegetation time-series analysis. Remote Sensing of Environment, 201, 34–46. https://doi. org/10.1016/j.rse.2017.08.008
- Peterson, P. M., Romaschenko, K., Arrieta, Y. H., & Saarela, J. M. (2014a). (2332) Proposal to conserve the name Sporobolus against Spartina, Crypsis, Ponceletia, and Heleochloa (Poaceae: Chloridoideae: Sporobolinae). Taxon, 63(6), 1373–1374. https://doi.org/10.12705/636.23
- Peterson, P. M., Romaschenko, K., Arrieta, Y. H., & Saarela, J. M. (2014b). A molecular phylogeny and new subgeneric classification of Sporobolus (Poaceae: Chloridoideae: Sporobolinae). Taxon, 63(6), 1212–1243. https://doi.org/10.12705/636.19
- Pezeshki, S. R., Pardue, J. H., & Delaune, R. D. (1993). The influence of soil oxygen deficiency on alcohol dehydrogenase activity, root porosity, ethylene production and photosynthesis in Spartina patens. Environmental and Experimental Botany, 33(4), 565–573. https://doi.org/10.1016/0098-8472(93)90031-A
- Porcar-Castell, A. (2011). A high-resolution portrait of the annual dynamics of photochemical and non-photochemical quenching in needles of Pinus sylvestris. Physiologia Plantarum, 143(2), 139–153. https://doi.org/10.1111/j.1399-3054.2011.01488.x
- Porcar-Castell, A., Pfundel, E., Korhonen, J. F. J., & Juurola, E. (2008). A new monitoring PAM fluorometer (MONI-PAM) to study the short- and long-term acclimation of photosystem II in field conditions. *Photosynthesis Research*, 96(2), 173–179. https://doi.org/10.1007/ s11120-008-9292-3
- Rossini, M., Meroni, M., Migliavacca, M., Manca, G., Cogliati, S., Busetto, L., et al. (2010). High resolution field spectroscopy measurements for estimating gross ecosystem production in a rice field. Agricultural and Forest Meteorology, 150(9), 1283–1296. https://doi.org/10.1016/j. agrformet.2010.05.011
- Schäfer, K. V. R., Tripathee, R., Artigas, F., Morin, T. H., & Bohrer, G. (2014). Carbon dioxide fluxes of an urban tidal marsh in the Hudson-Raritan estuary. Journal of Geophysical Research: Biogeosciences, 119, 2065–2081. https://doi.org/10.1002/2014/G002703
- Silva, J., Santos, R., Calleja, M. L., & Duarle, C. M. (2005). Submerged versus air-exposed intertidal macrophyle productivity: From physiological to community-level assessments. *Journal of Experimental Marine Biology and Ecology*, 317(1), 87–95. https://doi.org/10.1016/j.jembe.2004.11.010
- Smart, R. M. (1982). Distribution and environmental control of productivity and growth form of Spartina alterniflora (Loisel.). In D. N. Sen, & K. S. Rajpurohit (Eds.), Contributions to the ecology of halophytes (pp. 127–142). Springer.
- Sun, Y., Frankenberg, C., Wood, J. D., Schimel, D. S., Jung, M., Guanter, L., et al. (2017). OCO-2 advances photosynthesis observation from space via solar-induced chlorophyll fluorescence. Science, 358(6360), eaam5747. https://doi.org/10.1126/science.aam5747
- USDA, N. (2020). The plants database. National Plant Data Team. Retrieved from http://plants.usda.gov/
- Verma, M., Schimel, D., Evans, B., Frankenberg, C., Beringer, J., Drewry, D. T., et al. (2017). Effect of environmental conditions on the relationship between solar-induced fluorescence and gross primary productivity at an OzFlux grassland site. *Journal of Geophysical Research: Biogeosciences*, 122,716–733. https://doi.org/10.1002/2016JG003580
- Winkel, A., Colmer, T. D., & Pedersen, O. L. E. (2011). Leaf gas films of Spartina anglica enhance rhizome and root oxygen during tidal submergence. Plant, Cell and Environment, 34(12), 2083–2092. https://doi.org/10.1111/j.1365-3040.2011.02405.x
- Yang, H., Yang, X., Zhang, Y., Heskel, M. A., Lu, X., Munger, J. W., et al. (2017). Chlorophyll fluorescence tracks seasonal variations of photosynthesis from leaf to canopy in a temperate forest. Global Change Biology, 23(7), 2874–2886. https://doi.org/10.1111/gcb.13590

MAO ET AL. 16 of 17

Yang, X., Tang, J., Mustard, J. F., Lee, J.-E., Rossini, M., Joiner, J., et al. (2015). Solar-induced chlorophyll fluorescence that correlates with canopy photosynthesis on diurnal and seasonal scales in a temperate deciduous forest. Geophysical Research Letters, 42, 2977–2987. https://doi.org/10.1002/2015GL063201

Zhang, Y., Guanter, L., Berry, J. A., van der Tol, C., Yang, X., Tang, J., & Zhang, F. (2016). Model-based analysis of the relationship between sun-induced chlorophyll fluorescence and gross primary production for remote sensing applications. Remote Sensing of Environment, 187, 145–155. https://doi.org/10.1016/j.rse.2016.10.016

MAO ET AL. 17 of 17